

Fe-Cu-ZnO NANOCOMPOSITE AS NOVEL ADSORBENT: CHARACTERIZATIONS AND INDIGO CARMINE DYE REMOVAL

A. MODWI^{a,b*}

^a*Department of Chemistry, College of Sciences, Al Imam Mohammad Ibn Saud Islamic University (IMSIU)*

^b*Department of Chemistry, College of Science & Technology, Omdurman Islamic University, Omdurman*

Herein, the Fe-Cu-ZnO nanocomposites with superior adsorption property and short contact time were prepared by a sol-gel method. The structural characterizations were analyzed via several analytical techniques including X-ray powder diffraction (XRD), the surface area and pore distribution (BET) method, scanning electron microscopy (SEM), Energy Dispersive X-ray Spectrometer (EDX) and Thermogravimetric analysis (TGA). It was found that the nanocomposite with a diameter of 18nm and surface area of 63 m²/g. The adsorption of dye model was fitted well with Langmuir model and the adsorption capacity was 77.7mg.g⁻¹ at room temperature. The kinetics of adsorption rate of the indigo carmine was very fast, and fitted with a pseudo second order.

(Received April 21, 2018; Accepted July 3, 2018)

Keywords: Fe-Cu-ZnO nanocomposite; Characterizations; TGA; Contact time; adsorption capacity

1. Introduction

The existences of dyes in wastewater and groundwater are a worldwide trouble and have attracted great consideration. Industrial wastewater involves dangerous and refractory organic dyes pollutants causing severe environmental issues. One of the typical organic pollutant species, synthetic dyes such as methylene blue, malachite green and indigo carmine with a annual manufacturing of more than 700,000 tones are broadly used in textile, leather, paper, paint, plastic and other industries uses[1,2]. For the reason that of their complex molecular structures and large sizes most of the dyes are considered non oxidizable by conservative physical and biological removal [3]. A variety of process such as adsorption, solvent extraction, and photocatalysis has been employed to eliminate organic dyes from the wastewater [4-6]. Each of these methods has some merits and confines in perform. Adsorption using a nanomaterials with large surface area has proved to be one of the most candidate methods among of the above-mentioned process [7]. Nanomaterials adsorbents are generally effective in the removal and recovery of dyes because of their physical and chemical stabilities[8].

In the present article, we report on the successful fabrication of Fe-Cu-ZnO nanocomposite through a simple sol-gel method calcinated at 550 °C. The structural, morphology, surface properties and chemical stability of the Fe-Cu-ZnO sorbent were studied by various analytical techniques. Moreover, the kinetics and isotherms of the Fe-Cu-ZnO adsorbent for indigo carmine dye adsorption was investigated in order to investigate the contact time and adsorption capacity.

*Corresponding author: abuelizkh81@gmail.com

2. Experimental section

2.1. Synthesis of Fe-Cu-ZnO nanocomposite

In the typical fabrication, 4g of zinc acetate was dissolved in 75ml methanol with gently stirring at room temperature. Then, the required amount of copper nitrate and ferric nitrate were added to the zinc acetate methanol mixture under vigorous magnetic stirring. Afterward, the aqueous solution of tartaric acid was added drop wise to the mixture and the gel formed fast at room temperature. The gel was then dried at 85°C for 16 h and the obtained dry gel was first grounded and annealed at 550°C for 2 hour. All the chemicals used without further purification and the structure of the indigo carmine dye are demonstrated in Fig.1.

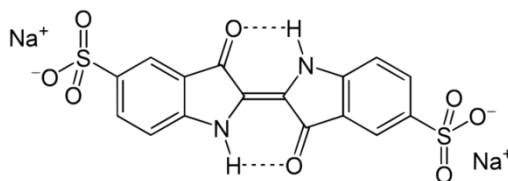


Fig.1. Indigo carmine structure.

2.2. Characterization techniques

The phase structure and crystallite size of nanocomposite was determined by the powder X-ray diffraction patterns, the compound was conducted on a diffractometer (D8 Advance Bruker) via Cu-K α radiation, $\lambda = 0.15406$ nm with accelerating voltage is 40kV and scanning angle is 20⁰-75⁰. The surface properties of nanocomposite were investigated using (BET) method recorded on a Micrometrics ASAP 2020 apparatus. The morphology of specimen was observed by a field emission scanning electron microscope (FE-SEM, JEOL-6700F). The elemental composition of Fe/Cu/ZnO composite was determined by energy dispersive X-ray spectrometer (EDX). The thermal decomposition behavior of sample was studied using Thermogravimetric (Model: Mettler Toledo) with a heating rate of 0.02 to 250 K/min, room temperature of 800°C and crucible volume of up to 150 μ L were utilized.

2.3. Adsorption kinetics and isotherms procedure

2.3.1 Adsorption Experiments details

The adsorption experiments were conducted to examine the adsorption parameter of the Indigo carmine dye on the synthesized Fe-Cu-ZnO nanocomposite. The equilibrium adsorption experiment was performed in 50 ml conical flasks containing 10 mg of nanocomposite and 20 ml of dye with concentrations 5, 15, 25, 35, 60 and 80 mg/L were added under magnetic stirrer for 60 min. Following adsorption equilibrium, the suspension nanomaterials was separated from the solution via centrifugation, and the residual dye concentration was determined using the spectrophotometer (Labomed – UVS-2800) at a maximum wavelength of 610 nm.

The adsorption kinetic investigation, the volume and initial concentration of dye were 200ml and 60mg/L respectively, and the mass of the Fe-Cu-ZnO was 100mg. The experiment was conducted in the dark under vigorous magnetic stirring. Afterwards, 5 ml of the suspension was withdrawn at predetermined time intervals, and centrifuged for measuring the residual dye concentration. The quantity of dye adsorbed per gram of catalysts at time (min) can be determined from the following equation [9]:

$$q_t = \frac{V(C_0 - C_t)}{m} \quad (1)$$

where, q_t (mg g⁻¹) is mass of dye adsorbed by a unit mass of nanopowder m (g) at time t (min), V is the solution volume (L), C_0 concentration of the metal ion initially preset and C_t is that at t time in (mg L⁻¹). At equilibrium, a similar formula is used to find out the mass adsorbed q_e :

$$q_e = \frac{V(C_0 - C_e)}{m} \quad (2)$$

Adsorption equilibrium experiment is usually modeled by adsorption isotherms. In particular Langmuir and Freundlich representations are the widely employed to describe the established equilibrium. They are symbolized in linear forms to make their graphical illustrations pertinent.

$$\frac{C_e}{q_e} = \frac{1}{q_m} C_e + \frac{1}{q_m \cdot K_L} \quad \text{Langmuir model equation} \quad (3)$$

$$\ln q_e = \frac{1}{n} \ln C_e + \ln K_F \quad \text{Freundlich model equation} \quad (4)$$

where q_m is the quantity of adsorbed solid-phase that accomplishes a monolayer treatment of adsorption sites and K_L is a parameter connected with the adsorption free energy [10]. q_m and K_L represent the slope and intercept of C_e/q_e versus C_e plotting. While k and n of Freundlich formula are obtained from the $\ln q_e$ versus $\ln C_e$ diagrams. K_F and n of the Freundlich model are correlated with the adsorptive bond strength and distribution, respectively [10].

Adsorption kinetics information is typically obtainable by a pseudo-second-order is modeled by equation (5), where k_2 denotes the rate constant (g (mg.min)^{-1}) [11]. Using of t/q_t against t graph, q_e and k_2 are correspondingly obtained from the slope and intercept.

$$\frac{t}{q_t} = \frac{1}{k_2 \cdot q_e^2} + \frac{t}{q_e} \quad (5)$$

3. Results and discussion

3.1. Characterization of the fabricated nanocomposite by X-ray diffraction

Fig. 2 displays the XRD spectra for Fe-Cu-ZnO nanocomposite synthesized through the sol-gel method. The findings show broad peaks at positions (31.61° , 34.39° , 36.11° , 47.40° , 56.52° , 62.72° , 66.29° , 67.91° and 69.08°) of the spectrum. These results of diffraction peaks agree with the wurtzite hexagonal ZnO standard data (JCPDS- 36-1451) in addition to a small peak at position 38.65° , corresponding to CuO monoclinic (111) base-centered phase JCPDS#18-1916. This additional peak at 111° could be due to the solubility of 5% Cu on ZnO is limits and resulted in high grain boundaries. The average diameters of crystallite (D) of the prepared nanocomposite was calculated using the Scherrer's equation [12]:

$$D = \frac{0.9 \lambda}{\beta \cos \theta} \quad (6)$$

here λ is the wavelength of Cu $K\alpha$ radiation is, β is the full width half maxima (FWHM) of the diffraction peak and θ is the Bragg peak angle. The crystallite size calculated from the Scherrer's equation is 18 nm for Fe-Cu-ZnO at 550°C . In literature, the crystallite sizes of pure ZnO decrease when it doping with low concentration of Cu ion, this chiefly qualified to the formation of Cu – O – Zn on the surface, which hinders the growth of crystal grains [13].

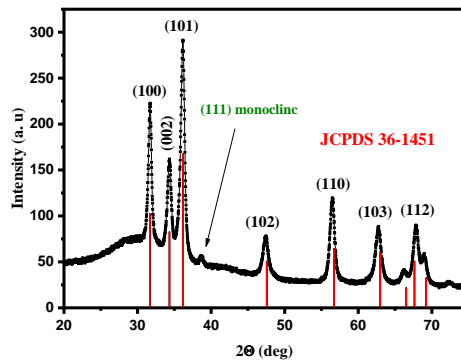


Fig.2.XRD pattern of nanocomposite.

3.2. Nitrogen Adsorption Analysis of Fe-Cu-ZnO nanomaterials

Fig. 3.demonstrates the nitrogen adsorption-desorption isotherms inset Barrett-Joyner-Halenda (BJH) pore size distribution for Fe-Cu-ZnO nanocomposite at the temperature 550°C. The isotherms obtained are Type IV related to a capillary condensation, according to the International Union for Pure and Applied Chemistry (IUPAC) classification. The hysteresis is Type H3 characteristics of the mesoporous material with slit-shape pores. Based on the results from (Fig.3).The surface area of nanocomposite was $63 \text{ m}^2\text{g}^{-1}$ with the pore volume and pore diameter $0.22\text{cm}^3/\text{g}$ and 9.82 nm respectively.

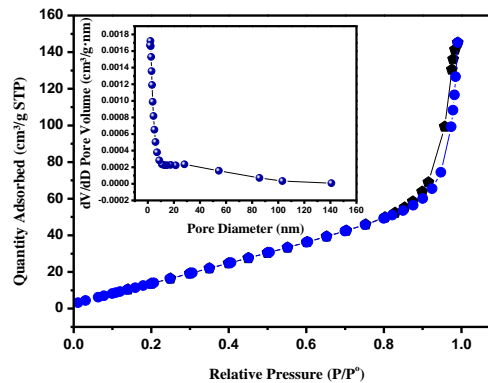


Fig.3. BET adsorption-desorption isotherms of composite.

3.3 Morphology and composition analysis

Fig. 4(a) depicts the SEM and EDX of the Fe-Cu-ZnO nanocomposite. The SEM image shows heterogeneity in the shapes and sizes of the particles that contain elongated shapes .Fig. 4(b) displays the EDX result of Fe-Cu-ZnO composite. The elemental composition percentage of the constituents of O, Zn, Cu and Fe in the composite is determined. The EDX finding confirms the stoichiometry of Fe, Cu, Zn and O lattice with their nominal percentage and the real incorporation of Cu and Fe in the ZnO matrix.

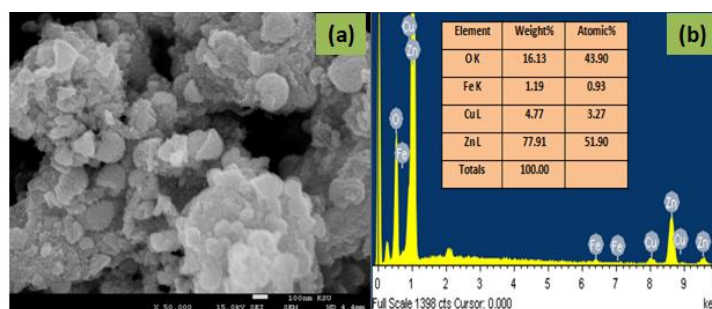


Fig.4. a) SEM image of a nanocomposite and b) EDX graph of a nanomaterials

3.4. Thermogravimetric (TGA) analysis and derivative

Fig.5 shows Thermogravimetric analysis (TGA) and derivative thermal gravimetric of composite xerogel was approved to explore the composite stability. The sample was heated from room temperature to 750 °C with an increase of 10 °C/min in atmosphere. Clearly, the TGA graph the weight loss of the nanocomposite is found to take place until 420°C. Furthermore, the DTG data plot three endothermic peaks are found at 246, 351 and 382°C. These peaks are due to water and organics evaporation. After 382°C, there is no additional weight loss of the compound.

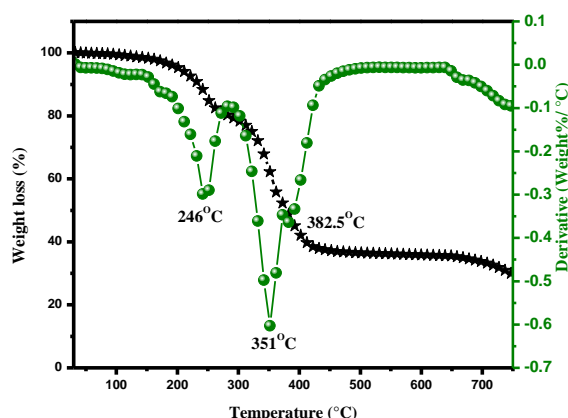


Fig. 5.TGA and DTG analysis for nanocomposites.

3.5. Kinetic study

Fig. 6(a) depicts the impact of contact time on the indigo carmine dye adsorption on the Fe-Cu-ZnO nanocomposite for different times at room temperature. It clearly demonstrated that the adsorption of dye varies proportionally with time reaching its maximum capacities q_t in 18 min. After that, the indigo carmine dye adsorption did not show a discrepancy with time increase. Thus, 18 min was considered the suitable time to reach equilibrium. Fig. 6(b) shows the pseudo-second-order model was exhibited a better fitting for the data ($r^2 = 0.9998$). Otherwise, the determined q_{\max} value is approximately equal $71.7 \text{ mg} \cdot \text{g}^{-1}$ from the experiments confirming a pseudo-second-order kinetics as shown in Table1.

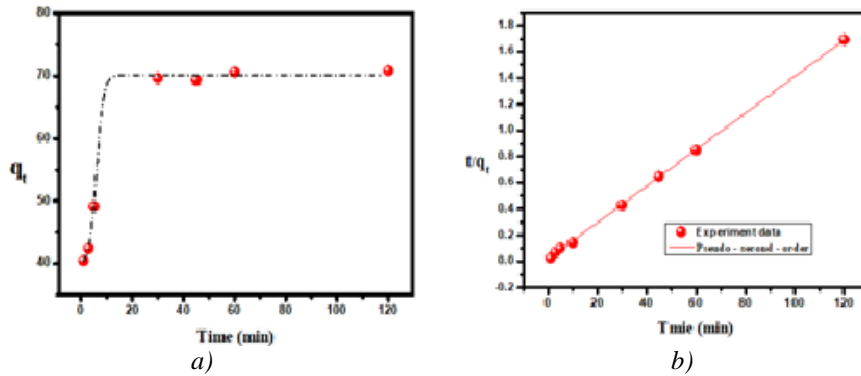


Fig.6. a) contact time and b) Pseudo-Second order kinetic model of dye adsorption on Fe-Cu-ZnO nanocomposite.

Table 1. Pseudo-Second order kinetic parameters for the dye adsorption by Fe-Cu-ZnO nanocomposite.

Pseudo-Second order kinetic parameters		
$k_f \times 10^{-2} (\text{min}^{-1})$	$q_e (\text{mg.g}^{-1})$	R^2
1.07	71.7	0.9998

3.6. Equilibrium study

The adsorption equilibrium whose parameters demonstrate the surface properties and affinity of the dye Indigo carmine on the Fe-Cu-ZnO nanocomposite was also scrutinized. Langmuir Fig.7(a) and Freundlich Fig.7(b) isotherms models, which are the most usually used, were employed to fit the experimental data [14,15]. The Langmuir adsorption model is depend on the postulation that maximum adsorption corresponds to a saturated monolayer of solute molecules without any interaction involving molecules on the adsorbent surface. As scheduled in Table 2, Langmuir isotherm provides better linear regression ($R^2 = 0.99$) than Freundlich equation ($R^2 = 0.97$), representing that the adsorption follows the Langmuir model. The indigo carmine adsorption capacity on Fe-Cu-ZnO nanocomposite at room temperature was 77.7 mg.g^{-1} . This results makes it a superior adsorbents compared those announced in the literature: Montmorillonite (40 mg.g^{-1}) [16], Cobalt hydroxide nanoparticles (62.5 mg.g^{-1})[17], Chitin nanowhisiker (ChNW)-functionalized abrasive spherical materials (0.4 mg g^{-1})[18], sewage sludge (60.04 mg g^{-1})[19], coal fly ash (1.48 mg g^{-1}) [20], zeolite from fly ash (1.23 mg g^{-1}) [20], mesoporous Mg/Fe layered double hydroxide nanoparticles (55.5 mg g^{-1}) [21].

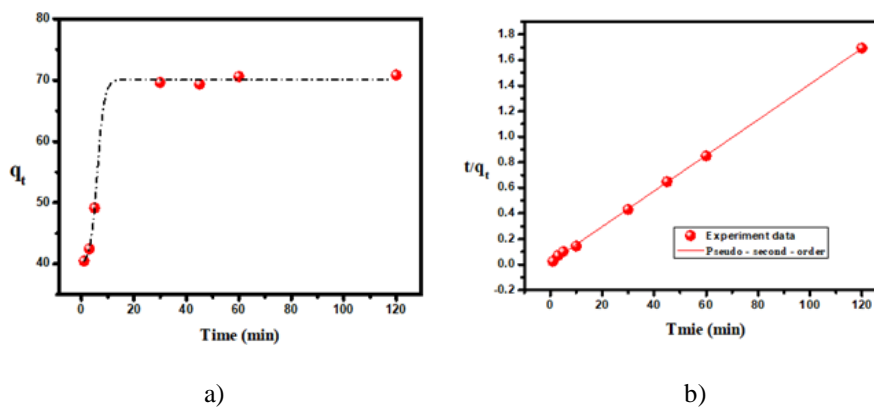


Fig. 7. a) Linear Langmuir and b) Linear Freundlich isotherms.

Table 2. Adsorption equilibrium constants for the dye on Fe/Cu/ZnO nanocomposite

Langmuir constants			Freundlich constants		
$q_m(\text{mg}\cdot\text{g}^{-1})$	$K_L(\text{l}\cdot\text{mg}^{-1})$	R^2	n	$\text{Ln } k_f$	R^2
77.7	0.188	0.990	1.82	1.90	0.975

4. Conclusions

To sum up that, the Fe-Cu-ZnO nanocomposite with a high surface area was prepared by using a simplistic sol-gel method and calcinated at 550°C. The nanocomposite showed a large surface area 63.32m²/g and crystallites size 18.48nm with a CuO phase in its crystalline structure. The nanocomposites showed good capacity for the adsorption of indigo carmine dye from aqueous solution at ambient room temperature. Additionally short contact time adsorption equal 18min. Finally, this nanocomposite can be promising and candidate for the elimination of indigo carmine dye in wastewater.

References

- [1] A. Ahmad, et al., RSC Advances **5**, 30801 (2015).
- [2] M.Sarvajith, G. K. K.Reddy, Y.Nancharaiah, Journal of Hazardous Materials **342**, 536 (2018).
- [3] B. K.Körbahti, A. Tanyolaç, Journal of Hazardous Materials **151**, 422 (2008).
- [4] A.Kausar, et al. Journal of Molecular Liquids **256**, 395 (2018).
- [5] P.Pandit, S.Basu, Environmental Science &Technology **38**, 2435 (2004).
- [6] M.Rauf, S. S.Ashraf, Chemical Engineering Journal **151**, 10 (2009).
- [7] I.Ghiloufi, J.El Ghoul, A.Modwi, L. El Mir, Materials Science in Semiconductor Processing **42**, 102 (2016).
- [8] K.Ozawa, S.Munakata, K.Edamoto, K.Mase, The Journal of Physical Chemistry C **115**, 21843 (2011).
- [9] A.Meng, J.Xing, Z.Li, Q.Li, ACS Applied Materials &Interfaces **7**, 27449 (2015).
- [10] Y.-H.Li, et al. Water Research **39**, 605 (2005).
- [11] L.Khezami, K. K. Taha, A. Modwi, Zeitschrift für Naturforschung A **72**, 409 (2017).
- [12] A. W.Burton, K.Ong, T.Rea, I. Y.Chan, Microporous and Mesoporous Materials **117**, 75 (2009).
- [13] R.Sharma, S.Patel, K. Pargaien, Advances in Natural Sciences: Nanoscience and Nanotechnology **3**, 035005 (2012).
- [14] S.Rengaraj, C. K.Joo, Y.Kim, J.Yi, Journal of Hazardous Materials **102**, 257 (2003).
- [15] T. A.Saleh, V. K.Gupta, Environmental Science and Pollution Research **19**, 1224 (2012).
- [16] F.Geyikçi, Progress in Organic Coatings **98**, 28 (2016).
- [17] J.Zolgharnein, M.Rastgordani, Journal of Molecular Liquids (2018).
- [18] C. N.Arenas, A.Vasco, M.Betancur, J. D. Martínez, Process Safety and Environmental Protection **106**, 224 (2017).
- [19] M.Otero, F.Rozada, L.Calvo, A.Garcia, A. Moran, Dyes and Pigments **57**, 55 (2003).
- [20] T. E.de Carvalho, D. A.Fungaro, C. P.Magdalená, P.Cunico, Journal of Radioanalytical and Nuclear Chemistry **289**, 617 (2011).
- [21] M.Ahmed, A. Mohamed, Chemosphere **174**, 280 (2017).